

# The effect of acids and bases on the dispersion and stabilization of ceramic particles in ethanol

Johnny Widegren<sup>a,\*</sup>, Lennart Bergström<sup>b</sup>

<sup>a</sup>Royal Institute of Technology, Department of Material Science and Engineering, SE-100 44 Stockholm, Sweden

<sup>b</sup>Institute for Surface Chemistry, PO Box 5607, SE-114 86 Stockholm, Sweden

Received 4 February 1999; received in revised form 5 July 1999; accepted 8 August 1999

## Abstract

The dispersion and stability of alumina, titania, and silicon carbide powders in ethanolic medium have been investigated. An operational pH-scale,  $\text{pH}^*$ , based on an ethanol-based reference electrode, was used to systematize the suspension properties. The electrokinetic behavior was determined as a function of  $\text{pH}^*$ . The isoelectric points in ethanol —  $\text{pH}_{\text{iep}}^*(\text{SiC})=7.5$ ;  $\text{pH}_{\text{iep}}^*(\text{Al}_2\text{O}_3)=4.4$  and  $\text{pH}_{\text{iep}}^*(\text{TiO}_2)=4.2$  — were discussed in relation to the dissociation constants of the charge determining reactions at the powder surfaces. We have evaluated the long-term stability of the ethanolic dispersions through settling studies which showed that the primary particle size could be retained for extended times providing that the surface potential and ionic strength were optimized. © 2000 Elsevier Science Ltd. All rights reserved.

**Keywords:**  $\text{Al}_2\text{O}_3$ ; Electrokinetic behaviour; Ethanol; SiC; Suspensions;  $\text{TiO}_2$

## 1. Introduction

Electrophoretic deposition (EPD) is a promising method for producing ceramic materials and composites with good control over layer thickness and interfacial smoothness.<sup>1–7</sup> Similar to other colloidal processing methods like pressure filtration and centrifugal casting, it is possible to minimize the flaw size and optimize the processing conditions for EPD by manipulating and controlling the interparticle forces.<sup>8</sup> EPD, which forms the green body from a relatively dilute suspension by applying a body force on the particles, has the potential to produce dense, homogeneous green bodies also from ultrafine particles. This makes EPD a prime candidate for producing nanocrystalline materials from powders. Nanocrystalline or nanostructured materials have attracted much interest because of the advantageous characteristics, e.g. higher fracture toughness, higher strength, lowered sintering temperature and improved magnetic properties.<sup>9–12</sup> For nanosized powders, the control of the electrokinetic properties and colloidal state of the suspension becomes even more essential because small variations in the range and magnitude of the interparticle forces may induce drastic changes in the particle packing and deposition behavior.

Colloidally stable ceramic suspensions can be obtained by creating a high charge density on the particle surface which results in a strong double-layer repulsion (electrostatic stabilization), or by adsorbing polymers on the particle surfaces where the interpenetration of the polymer layers generate a repulsive force, so-called polymeric or “steric” stabilization. Although electrostatic stabilization is considered most effective in aqueous medium, there is experimental evidence that a substantial surface charge density — with the associated counterion layer in solution — also can be created in ethanolic media.<sup>13,14,16</sup> Ethanol is the most common dispersion medium in EPD since aqueous based suspensions have the disadvantage of electrolysis.

The surface potential and the ionic strength in the solution are the two most important parameters controlling electrostatic stabilization in aqueous as well as nonaqueous media. In aqueous media, high surface charge densities, corresponding to high surface potentials, can be obtained by working far away from the point of zero charge ( $\text{pH}_{\text{pzc}}$ ) of the powder. A similar approach can be used also in non-aqueous media, providing that an operational pH scale ( $\text{pH}^*$ ) and thus an isoelectric point,  $\text{pH}_{\text{iep}}^*$ , for the specific solvent can be defined.<sup>16,32</sup> The ionic strength controls the range of the double-layer repulsion. Since low-dielectric-constant media have a low degree of electrolyte dissociation, the double-layer repulsion can be very long range resulting

\* Corresponding author.

in a slowly decaying potential.<sup>13</sup> Van der Hoeven and Lyklema showed that there should be enough ions in solution to render the potential decay around the particles steep, but there should not be such a high ion concentration that the van der Waals attraction overcomes the double layer repulsion.<sup>13</sup>

The objective of the present paper is to systematize the dispersion and stabilization of ceramic powders in ethanol. One of the investigated powders is nanometer-sized ( $\text{TiO}_2$ ), while the two others ( $\text{Al}_2\text{O}_3$  and  $\text{SiC}$ ) are in the submicrometer range. Different acids and bases were added to impart a surface charge at the powder/solvent interface. The effect of these acids and bases on the particle size, settling rate and electrokinetic properties were systematized by using an operational pH scale, which is related to an ethanol-based reference electrode providing a fast response in ethanolic suspensions.

## 2. Experimental

### 2.1. Powders and chemicals

We have studied three different powders:  $\text{Al}_2\text{O}_3$  (TM-DAR, Tamei Chemicals, Japan),  $\text{SiC}$  (MSC-20C, Mitsui Toatsu Chemicals, Japan) and  $\text{TiO}_2$  (Nanophase Technologies, USA). XRD studies (X'Pert System, Philips, The Netherlands) of the as-received powders show that the  $\text{Al}_2\text{O}_3$  powder is pure  $\alpha$ -phase and  $\text{SiC}$  is pure  $\beta$ -phase, while the  $\text{TiO}_2$  powder is a mixture of anatase and rutile. ESCA measurements (AXIS-HS, Kratos Analytical, UK) indicate that the powder surfaces do not contain any major impurities except for  $\text{SiC}$  that is covered with a  $\text{SiO}_2$  layer due to oxidation. The specific surface area was determined using single-point BET measurements with nitrogen as the adsorption molecule (Flowsorb II 2300, Micromeritics, USA). Table 1 summarizes the characteristics of the powders.

We used absolute ethyl alcohol (Kemetyl, Sweden) with a water level around 0.1%, determined by density measurements, as a solvent for all the suspensions. The additives used in this study are: Acetic acid (HAc), Citric acid, HCl 37% purum supplied by Kebo lab, LiOH 98%, Triethanolamine (TEA) and LiCl. If not mentioned elsewhere, the chemicals are manufactured by Merck and have pro analysi quality. All the additives, except HCl,

Table 1  
Physical characteristics of powders

	$\text{Al}_2\text{O}_3$	$\text{SiC}$	$\text{TiO}_2$
Major phases	Alfa	Beta	Anatase, rutile
Specific surface area ( $\text{m}^2/\text{g}$ )	14.7	15.5	45.0
Particle size <sup>a</sup> (nm)	210 (sedigraph)	150	28 (TEM)

<sup>a</sup> Data supplied by powder manufacturer.

were dried with molecular sieves overnight, to minimize the content of residual water.

### 2.2. pH measurements

We used a pH meter (Model 632, Metrohm, Switzerland) with a two-electrode set-up — an ordinary glass electrode for measurement and a separate double-junction reference electrode — for the pH measurements in ethanolic suspensions (Fig. 1). The reference electrode is a Ag–AgCl double-junction electrode in an electrolyte consisting of saturated LiCl in ethanol. Both chambers of the electrode are filled with the same saturated electrolyte. This choice of reference electrode makes the experimentally determined operational pH scale less sensitive to the water content in the solutions compared to using an aqueous-based reference electrode.<sup>15,17</sup> The liquid-junction potential during the measurement is minimized and the problem of leakage of water into the solution from the reference electrode is eliminated. One additional advantage of using an ethanol-based electrode is the time factor. It has been reported that measurements in ethanol solutions using a water-based reference electrode may result in a sluggish response, needing up to an hour to reach “steady state”.<sup>16</sup> The use of an ethanol-based reference electrode reduces this time considerably; steady state is reached within 15 min in pure ethanol ( $\text{pH}^* = 7.15$ ) and with additions on the mM level of acid or base, the time to steady state is well below 5 min. Unfortunately, there are no ethanolic-based buffers available. Therefore, the electrode set-up was calibrated using ordinary aqueous-based buffers, resulting in an operational pH scale.

### 2.3. Particle size measurements

Particle size measurements were used to study the effect of the acids and bases on the dispersion and colloidal

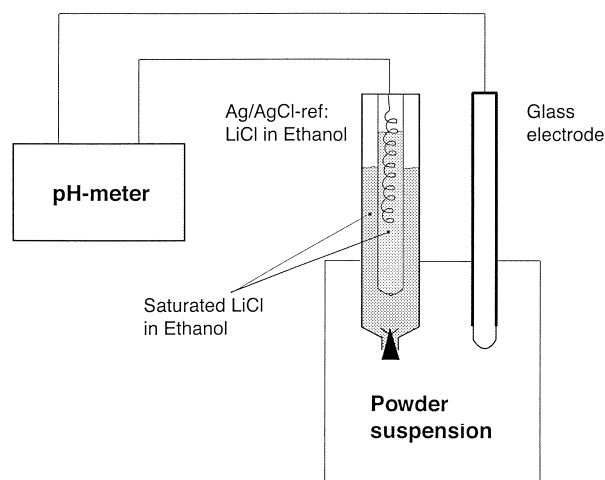


Fig. 1. Schematic figure describing the pH measurement set-up.

stability of the ethanolic suspensions. We used dynamic light scattering (Malvern Autosizer 2c, Malvern Instruments, UK) for the size measurements; a method suitable for particle sizes below 1  $\mu\text{m}$  with relatively narrow size distributions. All the size measurements were performed at room temperature ( $T \approx 20^\circ\text{C}$ ).

All powders were dried in a vacuum furnace containing phosphorus pentoxide as a drying agent prior to dispersion in order to minimize the water content on the powder surface. The pH was closely monitored during preparation of suspensions for the size measurements. Dried powder is mixed with ethanol and the 10 wt% mixture is shaken for 20 s. A small amount of the chosen additive is added to the suspension, pH is measured and the mixture is ultrasonically treated (Soniprep 150, MSE Scientific Instruments, UK) for 5 min to break up the agglomerates. We performed a separate study with acetic acid as additive to optimize the ultrasonication time. It was found that 5 min of ultrasonication was sufficient to reach a minimum in the particle size; for longer times, there is an increasing tendency for reagglomeration. After deagglomeration (ultrasonication), pH was measured and the suspension was diluted to a concentration of 200  $\text{g}/\text{m}^3$  suitable for light scattering measurements. This cycle is repeated with increasing additions of acid or base until no further decrease in particle size could be observed.

#### 2.4. Electrophoretic mobility

We used a Zetasizer IV (Malvern Instruments, UK) to measure the electrophoretic mobility. All measurements were done at  $20^\circ\text{C}$ . We added 0.5 mM LiCl to increase the conductivity ( $> 10 \mu\text{S}$ ), which improved the reproducibility of the electrokinetic measurements; it is very difficult to perform accurate and reproducible electrokinetic measurements in solutions of low conductivity since the electrical field may fluctuate and the current is too low.

The suspension preparation of samples for electrophoretic measurements followed a similar route as the preparation of samples for particle size analysis. A concentrated suspension (10 wt%) was deagglomerated using ultrasonication. From this concentrated suspension, a small sample is diluted to a concentration of 25  $\text{g}/\text{m}^3$ , acid (HCl or HAc) or base (LiOH or TEA) is then added followed by a 20 s shaking. The pH is measured before the sample was injected into the Zetasizer and the mobility was measured. This cycle involves a 5-min equilibration period between addition of additive and measurement of mobility. We typically covered the operational pH range from 2 to 10 by varying the amount acid or base added. To improve the reliability, we collected an average of 10 separate mobility measurements for each addition of acid or base.

### 3. Results and discussion

#### 3.1. Electrophoretic mobility

Electrophoretic mobility measurements were performed at a constant background electrolyte concentration consisting of 0.5 mM LiCl. The operational pH was controlled by the addition of acids (HCl and HAc) and bases (LiOH and TEA). The ionic strength is also an important parameter which is directly coupled to the extension of the double layer, expressed as the so-called Debye length,  $1/\kappa$ . The Debye length can be estimated by applying the Debye–Hückel approximation to the Poisson–Boltzmann resulting in

$$\kappa = (2ne^2z^2/\varepsilon_r\varepsilon_0k_B T)^{1/2} \quad (1)$$

where  $n$  is the ionic concentration,  $e$  is the electron charge,  $z$  is the valency of the ion-pair,  $\varepsilon_r$  and  $\varepsilon_0$  are the dielectric constant of the solvent and vacuum, respectively,  $k_B$  is the Boltzmann constant and  $T$  is the absolute temperature. This expression is also valid in low-polar and semi-polar media when a 1:1 electrolyte ( $z = 1$ ) is used.<sup>18</sup>

The experimental results from the mobility measurements are presented in Figs. 2–4 where both mobility and zeta potentials are reported. With the added electrolyte, we estimate  $\kappa a$  values on the order of 5–20 depending on particle size. We used the Henry equation<sup>31</sup>

$$u_E = \frac{2\varepsilon\zeta}{3\eta} \cdot f_1(\kappa a) \quad (2)$$

for calculating the zeta potential,  $\zeta$ , from the electrophoretic mobility,  $u$ ;  $\varepsilon$ ,  $\eta$  and  $f_1(\kappa a)$  are the dielectric constant, viscosity, and the Henry correction factor, respectively. This simple equation is accurate for systems having low zeta potentials ( $< 25 \text{ mV}$ ). For the higher  $\kappa a$  values (SiC and  $\text{Al}_2\text{O}_3$ ) the following expression for the Henry correction factor<sup>34</sup> was used:

$$f_1(\kappa a) = \frac{3}{2} - \frac{9}{2\kappa a} + \frac{75}{2\kappa^2 a^2} - \frac{330}{\kappa^3 a^3} \quad (3)$$

while, for the low  $\kappa a$  value ( $\text{TiO}_2$ ), we had to resort to a more complex expression

$$f_1(\kappa a) = 1 + \frac{(\kappa a)^2}{16} - \frac{5(\kappa a)^3}{48} - \frac{(\kappa a)^4}{96} + \frac{(\kappa a)^5}{96} - \left[ \frac{(\kappa a)^4}{8} - \frac{(\kappa a)^6}{96} \right] e^{\kappa a} \int_{\infty}^{\kappa a} \frac{e^{-t}}{t} dt \quad (4)$$

suggested by Henry.<sup>34</sup>

For all three powders, the zeta potential is positive at low operational pH values, crosses over to negative

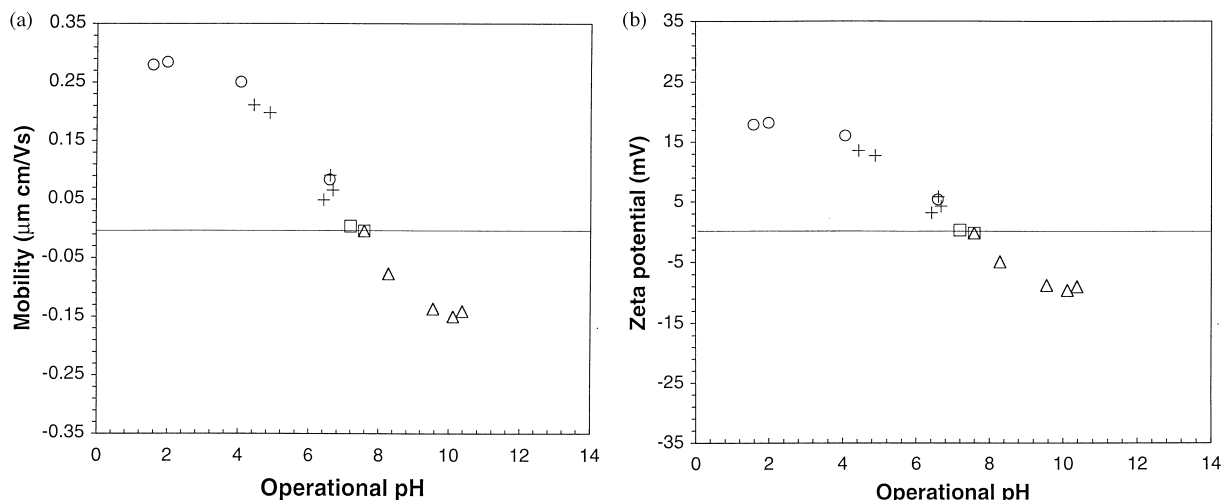


Fig. 2. (a) Electrophoretic mobility and (b) zeta potential of SiC in EtOH as a function of  $\text{pH}^*$ . Operational pH controlled with addition of; HCl (O), HAc (+), TEA ( $\square$ ); and LiOH ( $\Delta$ ).

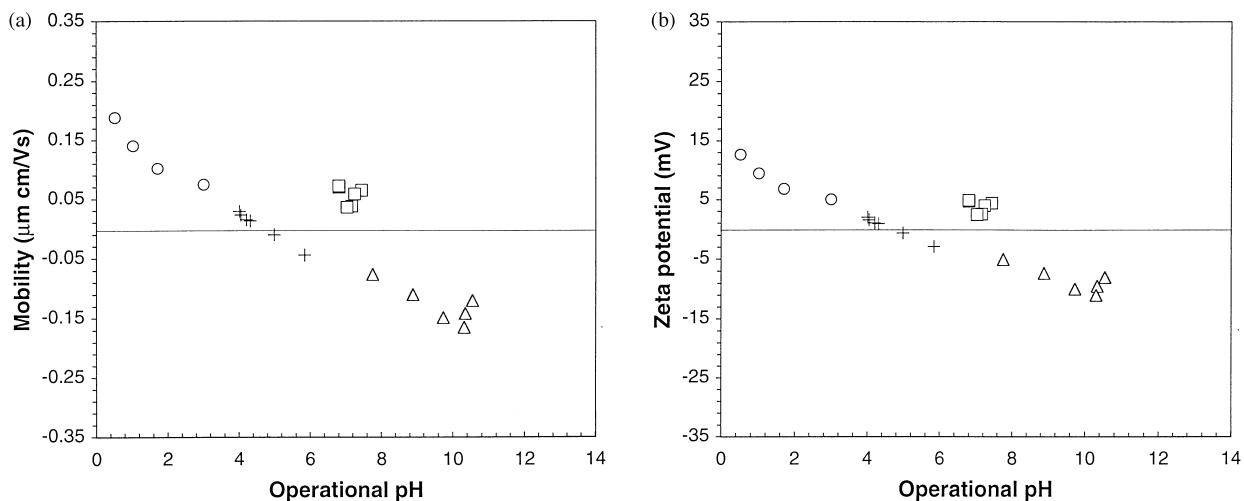


Fig. 3. (a) Electrophoretic mobility and (b) zeta potential of  $\text{Al}_2\text{O}_3$  in EtOH as a function of  $\text{pH}^*$ . Operational pH controlled with addition of; HCl (O), HAc (+), TEA ( $\square$ ); and LiOH ( $\Delta$ ).

values at a certain value which can be identified as the isoelectric point in ethanol ( $\text{pH}_{\text{iep}}^*$ ), and attains negative values at high  $\text{pH}^*$ . The mobility appears to be well defined by the operational pH except when triethanol amine (TEA) was used a base. TEA induces a substantially higher mobility compared to the general mobility– $\text{pH}^*$  curve for both alumina and titania (Figs. 3 and 4). This effect is probably caused by specific adsorption of TEA at the solid/liquid interface which induces a positive charge shifting the  $\text{pH}_{\text{iep}}^*$  to higher values. The magnitude of this effect depends on the affinity of the molecule to the surface and the concentration in solution.

Qualitatively, the  $\text{pH}^*$ -dependent electrokinetic behavior resembles the features of aqueous solutions where the site-dissociation reactions for an amphoteric oxide (MO) can be written as<sup>19</sup>



with each reaction characterized by a dissociation constant,  $K_a$ , in aqueous solutions defined as

$$K_{a1} = [\text{MO}^-]a_{\text{Hsurf}}/[\text{MOH}] \quad (7)$$

$$K_{a2} = [\text{MOH}]a_{\text{Hsurf}}/[\text{MOH}_2^+] \quad (8)$$

where  $a_{\text{Hsurf}}$  denotes the hydrogen ion activity at the surface (in aqueous solutions). At the  $\text{pH}_{\text{iep}}$ ,  $a_{\text{Hsurf}}$  equals the hydrogen activity in the bulk; when the surface is charged, however, a simple Boltzmann expression can be used to link the two activities. A similar set of dissociation constants can be defined in non-aqueous media

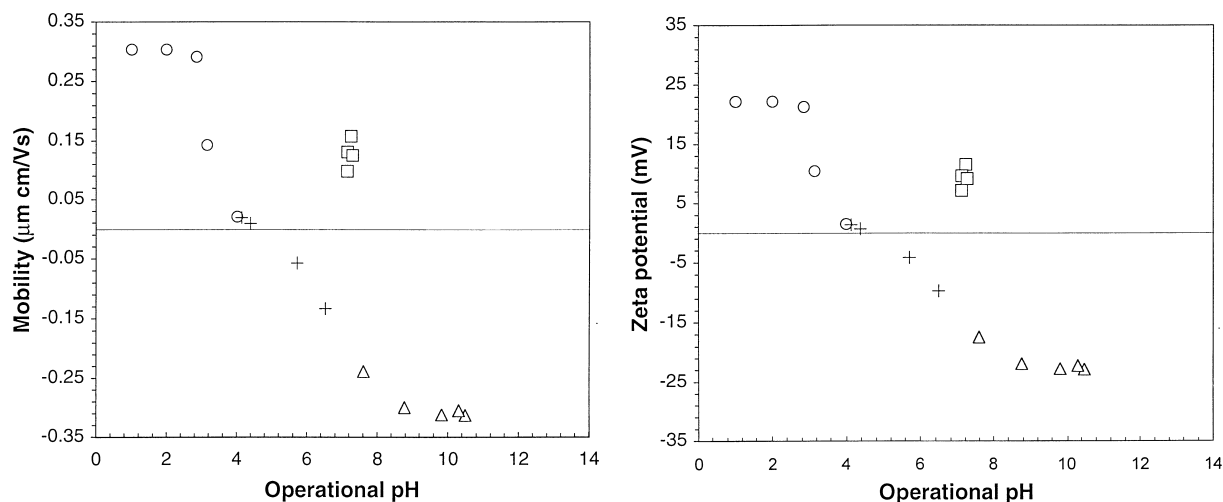


Fig. 4. (a) Electrophoretic mobility and (b) zeta potential of  $\text{TiO}_2$  in EtOH as a function of  $\text{pH}^*$ . Operational pH controlled with addition of: HCl (O), HAc (+), TEA (□); and LiOH ( $\Delta$ ).

$$K_{a1}^* = [\text{MO}^-]a_{\text{Hsurf}}^*/[\text{MOH}] \quad (9)$$

$$K_{a2}^* = [\text{MO}^-]a_{\text{Hsurf}}^*/[\text{MOH}_2^+] \quad (10)$$

It is easy to show that the isoelectric point is related to the dissociation constants according to

$$\text{pH}_{\text{iep}} = \text{p}K_{a1} + (\text{p}K_{a2} - \text{p}K_{a1})/2 \quad (11)$$

$$\text{pH}_{\text{iep}}^* = \text{p}K_{a1}^* + (\text{p}K_{a2}^* - \text{p}K_{a1}^*)/2 \quad (12)$$

for the aqueous and non-aqueous solutions, respectively. Comparing the isoelectric points in ethanol with the corresponding values in aqueous solutions suggests that there are large differences in dissociation behavior depending on media. The data for SiC (Fig. 2), displays an isoelectric point at  $\text{pH}_{\text{iep}}^* = 7.5$  which is substantially higher than the range determined previously in aqueous media ( $\text{pH}_{\text{iep}} = 2\text{--}5.5^{20\text{--}24}$ ). For the oxides, however, we obtain  $\text{pH}_{\text{iep}}^*$  values which are substantially lower than the corresponding values in aqueous solutions;  $\text{pH}_{\text{iep}}^* = 4.4$  for  $\text{Al}_2\text{O}_3$  and  $\text{pH}_{\text{iep}}^* = 4.2$  for  $\text{TiO}_2$  compared to  $\text{pH}_{\text{iep}}(\text{Al}_2\text{O}_3) = 8\text{--}9^{21,23\text{--}26}$  and  $\text{pH}_{\text{iep}}(\text{TiO}_2) = 5.5\text{--}7^{27\text{--}30}$ . Based on the differences in isoelectric point,  $\Delta\text{pH}_{\text{iep}} = \text{pH}_{\text{iep}} - \text{pH}_{\text{iep}}^*$ , the dissociation reactions appear to become more acidic for  $\text{Al}_2\text{O}_3$  and  $\text{TiO}_2$  but more basic for the oxidized SiC when the powders are immersed in ethanol compared to aqueous based suspensions.

Comparing our electrokinetic results on alumina with the previous study by Wang et al.,<sup>16</sup> we find some striking differences. They obtained a  $\text{pH}_{\text{iep}}^* = 7.1$  which is much higher than our value ( $\text{pH}_{\text{iep}}^* = 4.4$ ). This difference may be explained by the use of different electrode set-ups which precludes a direct comparison of the  $\text{pH}^*$  scales in the respective studies. Another possibility, however, is that the base — tetramethyl ammonium hydroxide (TMAH) — used by Wang et al.<sup>16</sup> adsorbs specifically onto the alumina surface, thus shifting the

$\text{pH}_{\text{iep}}^*$  to higher values. In a previous study, it was found that tetraethyl-ammonium ions adsorb specifically on silicon nitride in aqueous media thus increasing the isoelectric point with concentration.<sup>33</sup>

### 3.2. Colloidal stability

We have investigated the effect of acid and base additions on the colloidal stability by particle size measurements and settling rate studies. In these studies, no background electrolyte is used to resemble the conditions during EPD more closely. The optimum conditions for dispersing the powders are summarized in Table 2 where we report at what operational pH the minimum particle size is obtained using the different additives.

No additive is able to disperse all the powders in ethanol. One additive, citric acid, did not deagglomerate any powder to sizes below  $1\ \mu\text{m}$  for any amount of addition. We find that  $\text{TiO}_2$  and SiC can be dispersed in the acidic region, while  $\text{Al}_2\text{O}_3$  is dispersed at both acidic and basic  $\text{pH}^*$ . Comparing the values for  $\text{pH}^*$  at the optimum dispersion conditions with the electrokinetic data suggests that both SiC and  $\text{TiO}_2$  carry a positive charge in the well-dispersed condition. The  $\text{TiO}_2$  powder apparently acts as an acid itself and decreases the  $\text{pH}^*$  of the solution substantially; a 10 wt% solution of  $\text{TiO}_2$  in ethanol has a  $\text{pH}^* \approx 1$ . Hence, only a small amount of HAc is needed to disperse the powder. Somewhat surprising, the base TEA is also able to disperse the  $\text{TiO}_2$  powder. This effect is probably related to the specific adsorption of this additive which might induce a high positive charge at intermediate  $\text{pH}^*$  values. It is also possible that adsorbed TEA infers a short ranged steric repulsion that promotes the stability of the suspension of this nanosized powder.

Addition of a strong base, LiOH, and a strong acid, HCl, do not create a stable  $\text{TiO}_2$  suspension although the  $\text{pH}^*$

Table 2  
Operational pH and particle size at optimum addition of various acids and bases in ethanol suspensions<sup>a</sup>

Additives	Al <sub>2</sub> O <sub>3</sub>	SiC	TiO <sub>2</sub>
HAc	4.4/200	– <sup>b</sup>	0.1/90
HCl	–	0.1/270	–
TEA	7.6/240	–	1.9/70
LiOH	8.7/410	–	–

<sup>a</sup> pH\*/particle size (nm).

<sup>b</sup> Corresponds to agglomerated systems where the particle size never attains values smaller than 1000 nm.

values are sufficiently far away from pH<sub>iep</sub><sup>\*</sup>. Conductivity measurements suggest that these additives increases the ionic strength too much, thus compressing the double layer to such an extent that the attractive van der Waals forces induces flocculation. The poor stability of Al<sub>2</sub>O<sub>3</sub> upon addition of HCl can be explained by the same effect. Hence, optimum electrostatic stability can be obtained when the addition of acid or base shifts the pH<sup>\*</sup> sufficiently far away from pH<sub>iep</sub><sup>\*</sup> without increasing the ionic strength too much.

SiC is dispersed by addition of HCl; TEA is not an effective dispersant for this powder probably due to the absence of a strong specific interaction with the oxidized SiC surface. Alumina is deagglomerated by most of the additives. HAc and TEA, however, give the smallest particle size after deagglomeration. One major advantage with HAc is that the small particle size is retained over a wide range of addition. This is probably related to HAc being a weak acid; hence, only a fraction of the added acid actually dissociates and thus contribute to the ionic strength.

To complement the particle size measurements, we have investigated the colloidal properties at long times of some ethanolic suspensions by sedimentation rate measurements. The settling experiments were performed using the additives which have resulted in the smallest particle sizes for the respective powders; i.e. HCl for SiC, HAc and TEA for Al<sub>2</sub>O<sub>3</sub> and TiO<sub>2</sub>. We find that HCl cannot provide a long-time stability to SiC; the suspensions were unstable and settled within minutes. Hence, addition of this strong acid does not stabilize any of the three powders in ethanol, probably related to the high ionic strength.

In contrast, both the Al<sub>2</sub>O<sub>3</sub> and TiO<sub>2</sub> suspensions were stable for long times displaying the formation of a cloudy top layer which is typical for the settling of a colloidally stable, polydisperse powder. The settling rate curves (Fig. 5) were evaluated using Stokes equation:

$$d = \sqrt{\frac{v18\eta}{g(\rho - \rho_0)}} \quad (13)$$

where  $d$  is the particle diameter,  $\rho$  is the particle density,  $\rho_0$  is the density of the medium, and  $g$  is the gravitational acceleration. This equation is strictly valid only at infinite dilution; at higher solids loading, settling of the

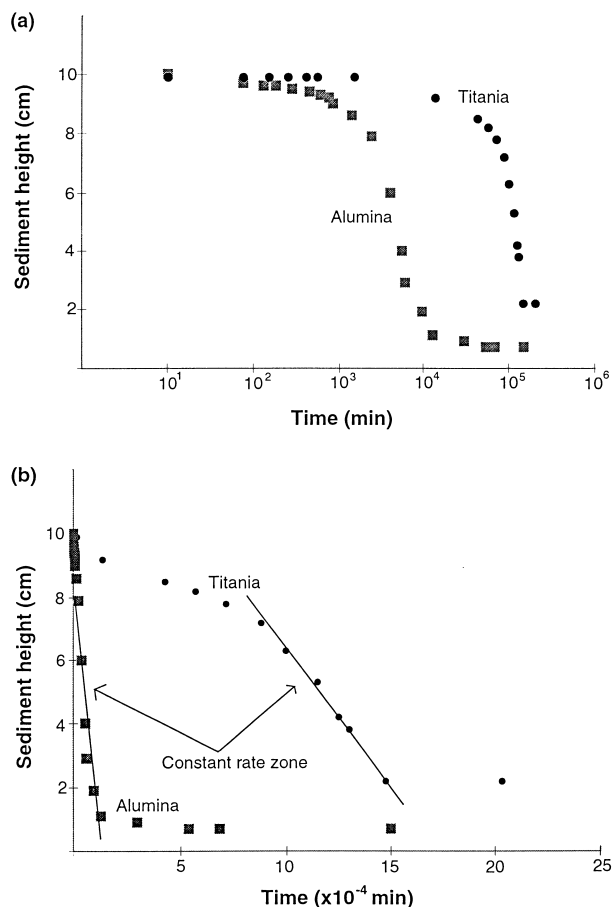


Fig. 5. Settling of Al<sub>2</sub>O<sub>3</sub> and TiO<sub>2</sub> in EtOH using HAc and triethanolamine as dispersing additives, respectively. Concentration is chosen for optimal dispersion, see Table 2. The data is plotted on (a) semi-logarithmic and (b) linear scale.

particles will be retarded by multi-body hydrodynamic effects. At the present solids loadings — 10 wt% which corresponds to 2–3 vol% — we expect the multi-body effects to be negligible.

We estimated the limiting settling rate,  $v$ , for the two systems from the constant rate zone in Fig. 5(b). Using these values,  $4.2 \cdot 10^{-4}$  cm/min and  $7.6 \cdot 10^{-5}$  cm/min, we calculate equivalent spherical diameters of 220 and 90 nm, for the alumina and titania particles, respectively. These estimates of the particle size from the settling studies corresponds very well with the light scattering measurements, indicating that the fine particle size is maintained over long times.

#### 4. Summary and conclusions

We have presented an electrode set-up — using an ethanol-based reference electrode — suitable for accurate and relatively fast measurements of the operational pH, pH<sup>\*</sup>, in ethanol-based solutions. The electrokinetic behavior was determined as a function of pH<sup>\*</sup>; we

obtained isoelectric points in ethanol,  $\text{pH}_{\text{iep}}^*$  that differed significantly from the isoelectric points in aqueous media. For SiC, we obtained  $\text{pH}_{\text{iep}}^* = 7.5$ ; for the oxides, we obtained  $\text{pH}_{\text{iep}}^* = 4.4$  for  $\text{Al}_2\text{O}_3$  and  $\text{pH}_{\text{iep}}^* = 4.2$  for  $\text{TiO}_2$ .

We have demonstrated that electrostatically stabilized suspensions of ceramic powders in ethanol can be obtained by tuning the operational pH and controlling the ionic strength. Adding an acid or base which shifts  $\text{pH}^*$  sufficiently far away from the  $\text{pH}_{\text{iep}}^*$  is generally able to disperse the primary particles and stabilize the suspension providing that the ionic strength (Debye length) is in the right range. We found that both  $\text{Al}_2\text{O}_3$  and  $\text{TiO}_2$  are stabilized over a relatively wide range of HAc addition, while SiC is best deagglomerated with controlled addition of HCl. Settling studies, however, showed that none of the additives can provide long-time stability to SiC; the suspensions were unstable and settled within minutes. A base, triethanolamine (TEA) is also able to stabilize both  $\text{Al}_2\text{O}_3$  and  $\text{TiO}_2$ , which we relate to the specific adsorption of TEA at the oxide/liquid interface.

The results in this investigation will form the base for future studies using EPD to manufacture laminated composites from ultrafine powders.

## Acknowledgements

The authors express their gratitude to the Swedish Research Council for Engineering Science (TFR) and the Brinell Centre for funding this work. We also like to thank Marie Ernstsson, Institute for Surface Chemistry, for help with the ESCA measurements and David Rowcliffe, Department of Material Science and Engineering, KTH, for fruitful discussions.

## References

- Sarkar, P. and Nicholson, P. S., Electrophoretic deposition (EPD): mechanisms, kinetics, and application to ceramics. *J. Am. Ceram. Soc.*, 1996, **79**, 1987–2002.
- Zhang, Z., Huang, Y. and Jiang, Z., Electrophoretic deposition forming of SiC-TZP composite in a nonaqueous sol media. *J. Am. Ceram. Soc.*, 1994, **77**, 1946–1949.
- Koura, N., Tsukamoto, T., Shoji, H. and Hotta, T., Preparation of various oxide films by an electrophoretic deposition method: a study of the mechanism. *Jpn. J. Appl. Phys.*, 1995, **34**, 1643–1647.
- Powers, R. W., The electrophoretic forming of beta-alumina ceramics. *J. Electrochem. Soc.*, 1975, **122**, 490–500.
- Krishna Rao, D. U. and Subbarao, E. C., Electrophoretic deposition of magnesia. *Bull. Amer. Ceram. Soc.*, 1979, **58**, 467–469.
- Sarkar, P., Haug, X. and Nicholson, P. S., Structural ceramic microlaminates by electrophoretic deposition. *J. Am. Ceram. Soc.*, 1992, **75**, 2907–2909.
- Jean, Jau-Ho., Electrophoretic deposition of  $\text{Al}_2\text{O}_3$ -SiC composite. *Mat. Chem. Phys.*, 1995, **40**, 285–290.
- Lange, F. F., Powder processing science and technology for increased reliability. *J. Am. Ceram. Soc.*, 1989, **72**, 3–15.
- Niihara, K., and Nakahira, A., Particulate strengthened oxide nanocomposites. In *Advanced Structural Inorganic Composites*, ed. Vincenzini. Elsevier Science Publishers, London, 1990, pp. 637–664.
- Balachandran, U., Siegel, R. W., Liao, Y. X. and Askew, T. R., Synthesis, sintering, and magnetic properties of nanophase  $\text{Cr}_2\text{O}_3$ . *NanoStructured Materials*, 1995, **5**, 505–512.
- Gleiter, H., Nanostructured materials: state of the art and perspective. *NanoStructured Materials*, 1995, **6**, 3–14.
- Sternitzke, M., Review: structural ceramic nanocomposites. *J. Eur. Ceram. Soc.*, 1997, **17**, 1061–1082.
- van der Hoeven, Ph.C. and Lyklema, J., Electrostatic stabilization in non-aqueous media. *Adv. Colloid Interface Sci.*, 1992, **42**, 205–277.
- Parfitt, G.D., and Peacock, J., Stability of colloidal dispersions in non-aqueous media. In: *Surface and Colloid Science*, Vol. 10, ed. E. Matijevic. Plenum, New York, 1978, pp. 163–226.
- Bates, R. G., *Determination of pH, Theory and Practice*. Wiley, New York, 1965.
- Wang, G., Sarkar, P. and Nicholson, P., Influence of acidity on the electrostatic stability of alumina suspension in ethanol. *J. Am. Ceram. Soc.*, 1997, **80**, 965–972.
- Galster, H., *pH Measurement: Fundamentals, Methods, Applications, Instrumentation*. VCH, Weinheim, 1991.
- Ohshima, H. and Furusawa, K. (eds), *Electrical Phenomena at Interfaces; Fundamentals, Measurements and Applications*, 2nd edn. Marcel Dekker, New York, 1998.
- Hunter, J. R., *Foundations of Colloid Science*, Vol. I. Clarendon Press, Oxford, 1987.
- Kennedy, T., Poorteman, M., Cambier, F. and Hampshire, S., Silicon nitride-silicon carbide nanocomposites prepared by water processing of commercially available powders. *J. Euro. Ceram. Soc.*, 1997, **17**, 1917–1923.
- Baklouti, S., Pagnoux, C., Chartier, T. and Baumard, J. F., Processing of aqueous  $\alpha$ - $\text{Al}_2\text{O}_3$ ,  $\alpha$ - $\text{SiO}_2$  and  $\alpha$ -SiC suspensions with polyelectrolytes. *J. Eur. Ceram. Soc.*, 1997, **17**, 1387–1392.
- Sakka, Y., Bidinger, D. D. and Aksay, I., Processing of silicon carbide-mullite-alumina nanocomposites. *J. Am. Ceram. Soc.*, 1995, **78**, 479–486.
- Pugh, R. J. and Bergström, L., The uptake of Mg(II) on ultrafine  $\alpha$ -silicon carbide and  $\alpha$ -alumina. *J. Coll. Int. Sci.*, 1988, **124**, 570–580.
- Hashiba, M., Okamoto, H., Nurishi, Y. and Hiramatsu, K., The zeta-potential measurement for concentrated aqueous suspension by improved electrophoretic mass transport apparatus — application to  $\text{Al}_2\text{O}_3$ ,  $\text{ZrO}_3$  and SiC suspensions. *J. Mat. Sci.*, 1988, **23**, 2893–2896.
- Sprycha, R., Electrical double layer at alumina/electrolyte interface: I. Surface charge and zeta potential. *J. Coll. Int. Sci.*, 1989, **127**, 1–11.
- Cesarano III, J., Aksay, I. A. and Bleier, A., Stability of aqueous  $\alpha$ - $\text{Al}_2\text{O}_3$  suspensions with poly(methacrylic acid) polyelectrolyte. *J. Am. Ceram. Soc.*, 1988, **71**, 250–255.
- Barringer, E. A., The synthesis, interfacial electrochemistry, ordering, and sintering of monodisperse  $\text{TiO}_2$  powders. Ph.D. thesis, Materials Science Department, MIT, Cambridge, MA, 1984.
- Yates, D. E. and Healy, T. W., Titanium dioxide-electrolyte interface. *Faraday I.*, 1980, **76**, 9–18.
- Wiese, G. R. and Healy, T. W., Adsorption of Al(III) at the  $\text{TiO}_2$ - $\text{H}_2\text{O}$  interface. *J. Coll. Int. Sci.*, 1975, **51**, 434–442.
- Parks, G. A., The isoelectric points of solid oxides, solid hydroxides, and aqueous hydroxo complex systems. *Chem. Rev.*, 1965, **65**, 177–198.
- Hunter, J. R., *Zeta Potential in Colloid Science*. Academic Press, New York, USA, 1981.
- Kosmulski, M. and Matijevic, E.,  $\xi$ -Potentials of silica in water-alcohol mixtures. *Langmuir.*, 1992, **8**, 1060–1064.
- Bergström, L. and Pugh, R. J., Interfacial characterization of silicon nitride powders. *J. Am. Ceram. Soc.*, 1989, **72**, 103–109.
- Henry, D. C., The cataphoresis of suspended particles. Part I. — The equation of cataphoresis. *Proc. Roy. Soc. London.*, 1931, **A133**, 106–129.